PORE PRESSURE EFFECT ON COMPRESSIVE STRENGTH
OF LOW POROSITY ROCKS

Supattra Khamrat, Decho Phueakphum and Kittitep Fuenkajorn

School of Geotechnology, Institute of Engineering, Suranaree University of Technology,

Muang District, Nakhon Ratchasima, Thailand 30000

Phone (66-44) 224-758, Fax (66-44) 224-448

E-mail: kittitep@sut.ac.th

Abstract

The objective of this study is to experimentally determine the effects of pore pressures on the compressive strengths of Tak granite, Lopburi marl and Lopburi marble. Failure strengths are determined for various stress rates and confining pressures both under dry and saturated conditions. The applied axial stresses are controlled at constant rates of 0.001, 0.01, 0.1, 1.0 and 10 MPa/s. The confining stresses are maintained at 0, 3, 7, to 12 MPa using a polyaxial load frame. The specimens are prepared to obtain rectangular blocks with nominal dimensions of 50×50×100 mm³. The results indicate that the strengths of the saturated specimens are lower than those of the dry specimens, particularly under high confining pressures and high loading rates. The elastic modulus of dry specimens is higher than that of the saturated specimens. Based on the Coulomb criterion, the cohesions of the dry and saturated specimens are comparable. The dry specimens yield slightly higher friction angles than the saturated specimens. The distortional strain energy density required to fail the low porosity rocks under dry condition is slightly higher than that under saturated condition.

1. Introduction

The compressive strength and deformability of rocks are important parameters for the design and stability analysis of geologic structures. The effects of stress rate on the compressive strength and elastic modulus of rocks have long been recognized. It has been found that rock compressive strength and deformation modulus decrease with the loading rate [1-4]. Pore pressure has also been known as one of the factors lowering the rock strengths [5-8]. The rock compressive strengths decrease significantly as the water content increases. The measurement of pore pressure and its effect on the strength and deformability of low porosity rocks is however very difficult. The influence of water on deformability of rocks is also reflected as a reduction of Young's modulus and increase of Poisson's ratio, which indicates that the saturated rocks will deform more than the dry ones under the same stress condition [9-11].

The objective of this study is to experimentally determine the effects of pore pressures on the compressive strengths of granite, marl and marble. The rock strengths are determined for various stress rates and confining pressures both under dry and saturated conditions. This is primarily to indirectly reveal the effects of pore pressure on the mechanical behavior of low porosity and low permeability rocks. The distortional strain energy density at failure is determined to describe the rock strength as a function of mean strain energy.

2. Sample Preparation

The rock samples used in this research are Tak granite, Lopburi marl and Lopburi marble. The specimens have been prepared to obtain rectangular blocks with nominal dimensions of $50 \times 50 \times 100$ mm^3 for the uniaxial and triaxial compression tests. A minimum of 40 specimens are prepared for each rock types. The specimens are cut and ground to obtain the perpendicularity and parallelism to comply with the ASTM standard practice [12]. They are prepared to test under dry and fully saturated conditions. Under dry condition the specimen are over dried for 24 hours before testing. Under saturated condition the specimens are submerged under water in pressure vacuum chamber for 24 hours in order to saturate the specimens (Figure 1). The granite, marl and marble have average water contents (w) of 0.14%, 2.71% and 0.09%, respectively (Figure 2).

3. Test Method

The laboratory testing includes uniaxial and triaxial compression tests. Loading rates vary from 0.001, 0.01, 0.1, 1 to 10 MPa/s. A polyaxial load frame [13] is used to apply confining pressures from 0, 3, 7 to 12 MPa (Figure 3). The sample preparation, test methods and calculation follow relevant ASTM standard practices. The elastic modulus and compressive strength are measured. Neoprene sheets are used to minimize the friction at all interfaces between the loading plate and the rock surface. The tests are performed by increasing the axial stress to the rock specimen. The axial and
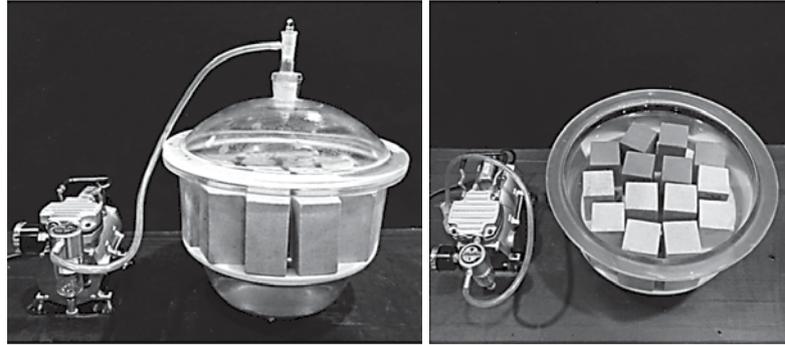
Figure 1 Sandstone specimens submersed under water in vacuum chamber.
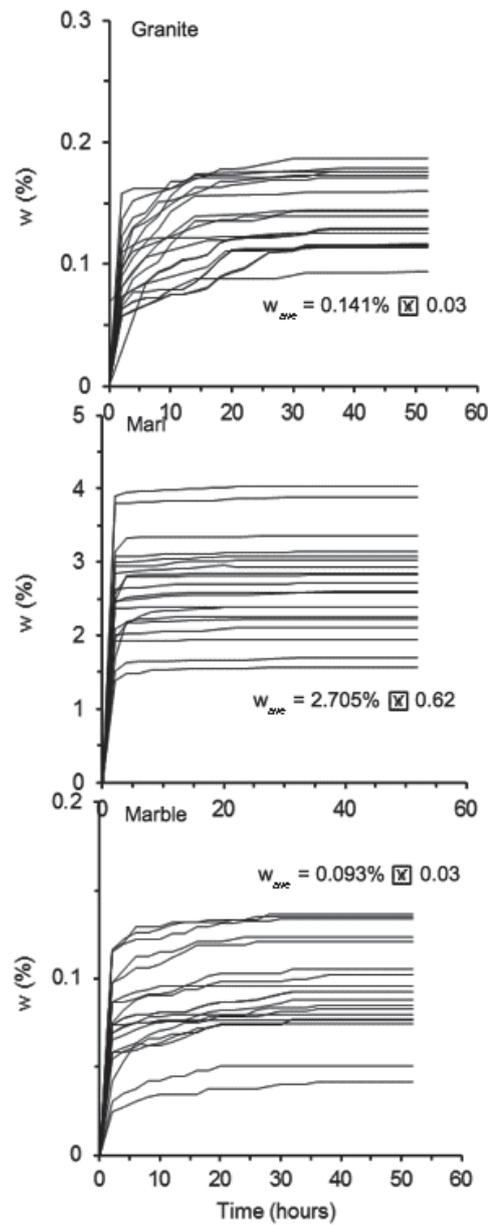

Figure 2 Water contents as function of time.

lateral strains are measured as a function of time until failure occurs. The dial gages are installed to measure the axial and lateral strains. During the test, the axial strain, lateral strain, and time are monitored.

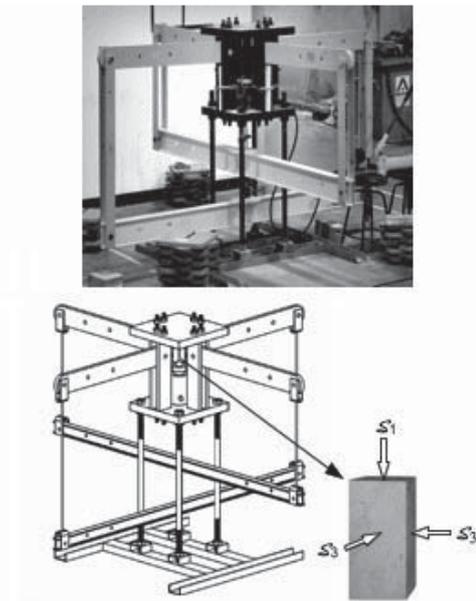**igure 3** Polyaxial load frame used in this study.

Figure 3   Polyaxial load frame used in this study.

4.   Test Results

Figure 4 shows some post-test marble specimens from the triaxial compression test under confining pressures (s_3) from 0, 3, 7 to 12 MPa with loading rates (s_1/t) of 1 and 0.001 MPa/s for both dry and saturated conditions. Post-test observations indicate that under high loading rates, the specimens fail by extension failure mode. Under low loading rates shear failure mode is observed.
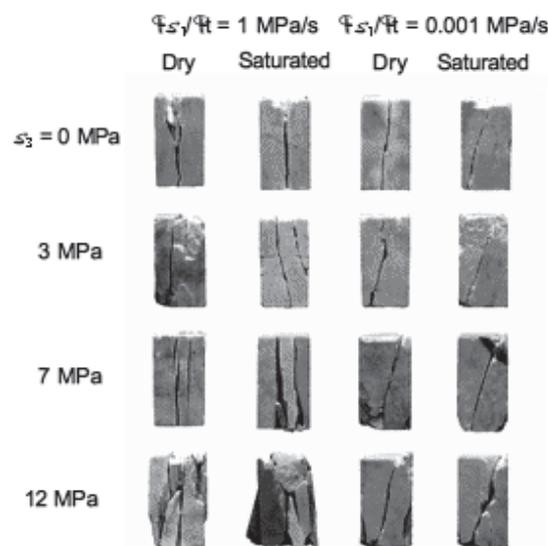

Figure 4 Some post-test marble specimens

4.1 Strength properties

The strengths of the saturated specimens are lower than those of the dry specimens, particularly under high confining pressures and high loading rates. Figure 5 shows the maximum principal stress $(s_{1,f})$ as a function of the applied loading rates.
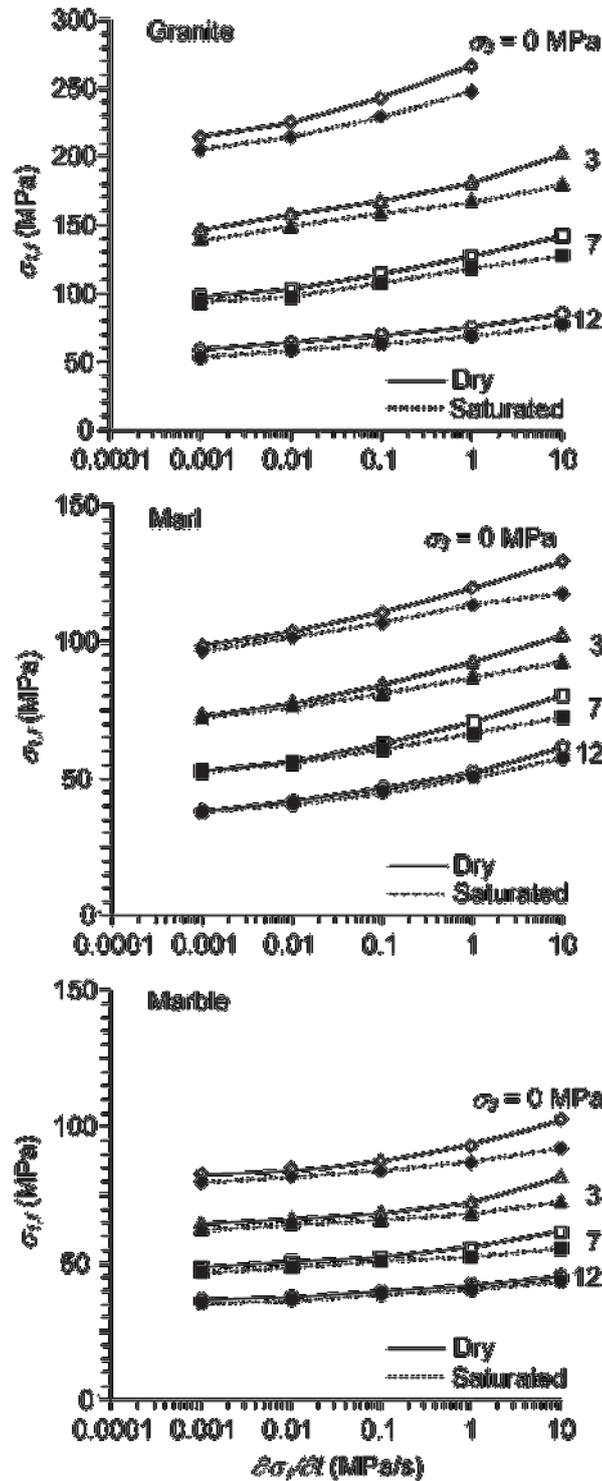

Figure 5 Maximum principal stress as a function of applied loading rate for dry and saturated specimens.

Based on the Coulomb strength criterion the cohesion and internal friction angle of the rocks have been calculated. The cohesions of the dry and saturated specimens are comparable (Figure 6). The dry specimens yield slightly higher friction angles than the saturated specimens (Figure 7). The shear strength (τ) can be represented by:

$$\tau = c + \sigma_n \, tan\phi \tag{1}$$

where σ_n is the normal stress, c is the cohesion and ϕ is the friction angle. They can be determined as a function of the stress rate as follows (Figures 6 and 7):

$$c = \chi \cdot ln(\partial\sigma_l/\partial t) + \psi \tag{2}$$

$$\phi = \omega \cdot ln(\partial\sigma_l/\partial t) + \iota \tag{3}$$

The parameters $\chi, \gamma, \omega, \iota$ are empirical constants.
Substituting equations (2) and (3) into (1) the shear strength of rocks can be presented as a function of stress rate:

$$\tau = [\; \chi \cdot ln(\partial\sigma_l\partial t) + \psi] + \sigma_n \, tan \, [\omega \cdot ln(\partial\sigma_l\partial t) + \iota] \quad (4) \tag{4}$$

4.2 Elastic parameters.

The elastic modulus (E) and Poisson's ratio (ν) are determined from the tangent of the stress–strain curves at 50% failure. The elastic modulus of the rock increases with loading rate (Figure 8). The influence of pore pressure on the rock deformability is reflected as the reduction of the Young's modulus. The Poisson's ratios of saturated specimens are slightly higher than those of the dry ones, and tend to be independent of the loading rate (Figure 9). Under lower loading rate of 0.001 MPa/s the elastic and Poisson's ratio under dry and saturated condition are similar. This suggests that the pore pressure has no effect on the rock strengths if there is sufficient time to allow water to flow out of the specimens. The elastic parameters can be best represented by:
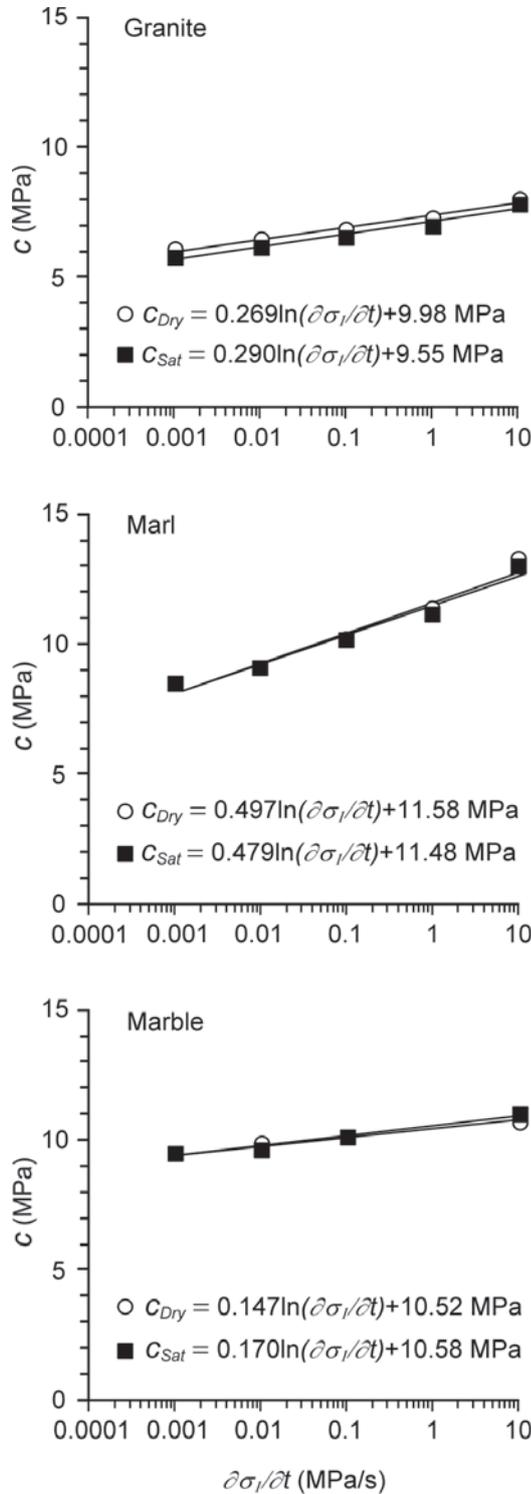
$$E = \kappa(\partial\sigma_l/\partial t)^\xi \tag{5}$$

Figure 6 Cohesion as a function of applied loading rate for dry and saturated specimens.

$$v = \alpha \ln\left(\partial\sigma_1/\partial t\right) + \beta \qquad\qquad (6)$$

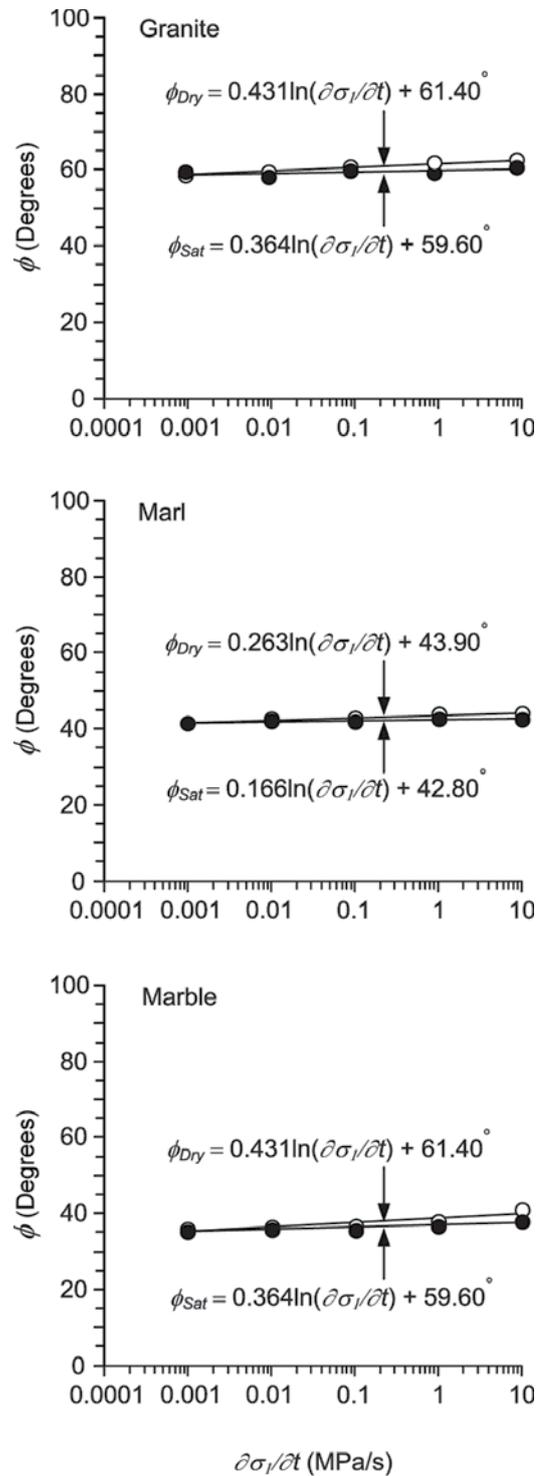The parameters $\kappa, \xi, \alpha, \beta$ are empirical constants.

Figure 7 Friction angle as a function of applied loading rate for dry and saturated specimens.

4.3 Strain energy density criterion.

The strain energy density principle is applied here to describe the rock strength and deformation under different loading rates. The distortional strain energy (W_d) at failure can be calculated from the shear modulus and octahedral shear stresses for each rock specimen as follows [14]:
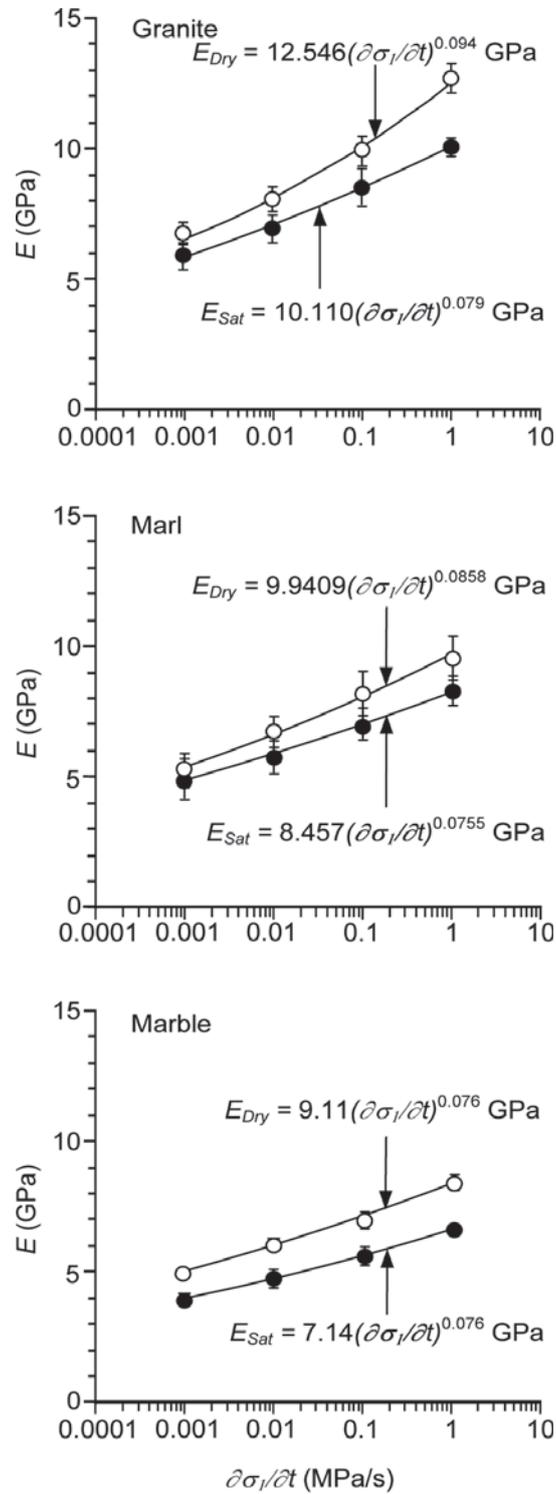
Figure 8 Elastic modulus as a function of applied loading rate for dry and saturated specimens.

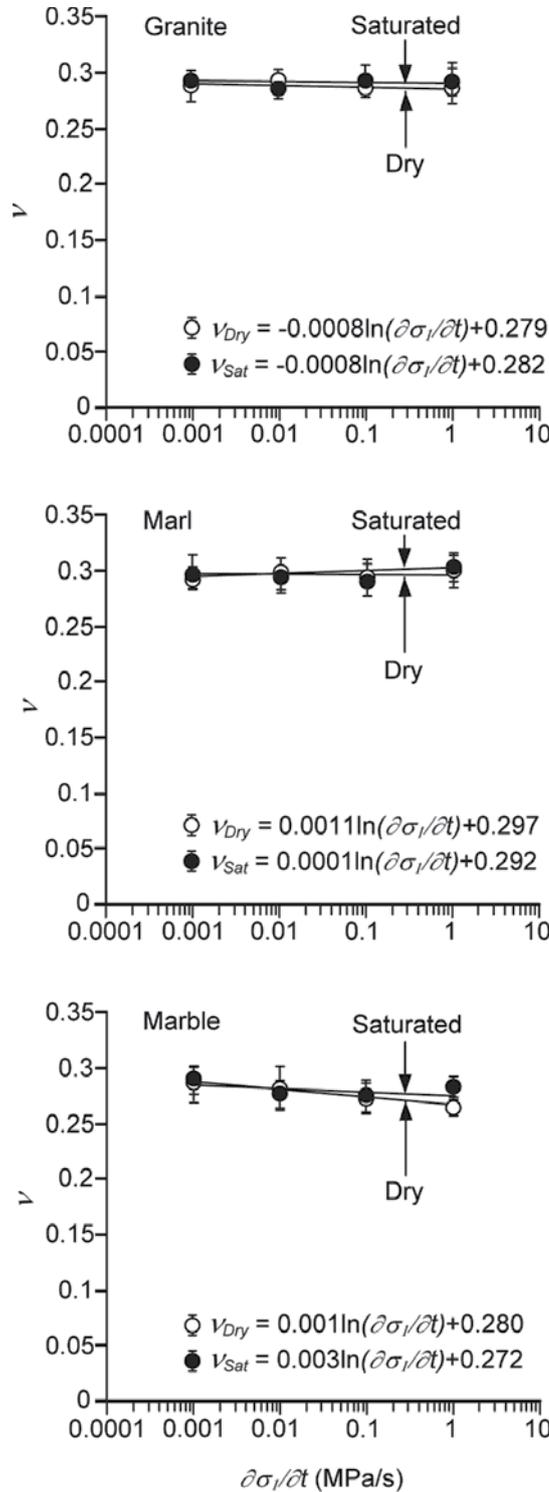$$W_d = \frac{3}{4}\left(\frac{\tau^2_{oct,f}}{G}\right) \tag{7}$$

Figure 9 Poisson's ratio as a function of applied loading rate for dry and saturated specimens.

The mean strain energy (W_m) at failure can also be derived as a function of the bulk modulus and mean stress at failure.

$$W_m = \left(\frac{\sigma^2_m}{2K}\right) \tag{8}$$

The elastic parameters G and K can be determined for each specimen using the following relations:

$$G = \frac{E}{2(1+v)} \tag{9}$$

$$K = \frac{E}{3(1-(2v))} \tag{10}$$

Regression on the test results shows that the distortional strain energy increases linearly with the mean strain energy for dry and saturated conditions (Figures 10 and 11) which can be best represented by:

$$W_d = \lambda W_m + \upsilon \tag{11}$$

The parameters l and u are empirical constants. The strain energy criterion gives an advantage that both stress and strain at failure are incorporated to define the point at which the rock can absorb the maximum energy before failure occurs.

5. Discussions and Conclusions

The results indicate that the granite, marl and marble have average water contents of 0.14%, 2.71% and 0.09%, respectively. The strengths of the saturated specimens are lower than those of the dry specimens, particularly under high confining pressures and high loading rates. This is because under low loading rates the rock specimens are subject to the consolidated drained condition as the pore water has sufficient time to seep out from the specimens. Under high loading rates however the specimens are subject to the consolidated undrained condition where the trapped pore water builds up the pore pressure and reduces the total failure stresses of the rocks. The elastic modulus of dry specimens is higher than that of the saturated specimens. A power equation can be used to describe the increase of the elastic modulus with the loading rate. The Poisson's ratios of saturated specimens are slightly higher than the dry specimens and tend to be independent of the loading rate.
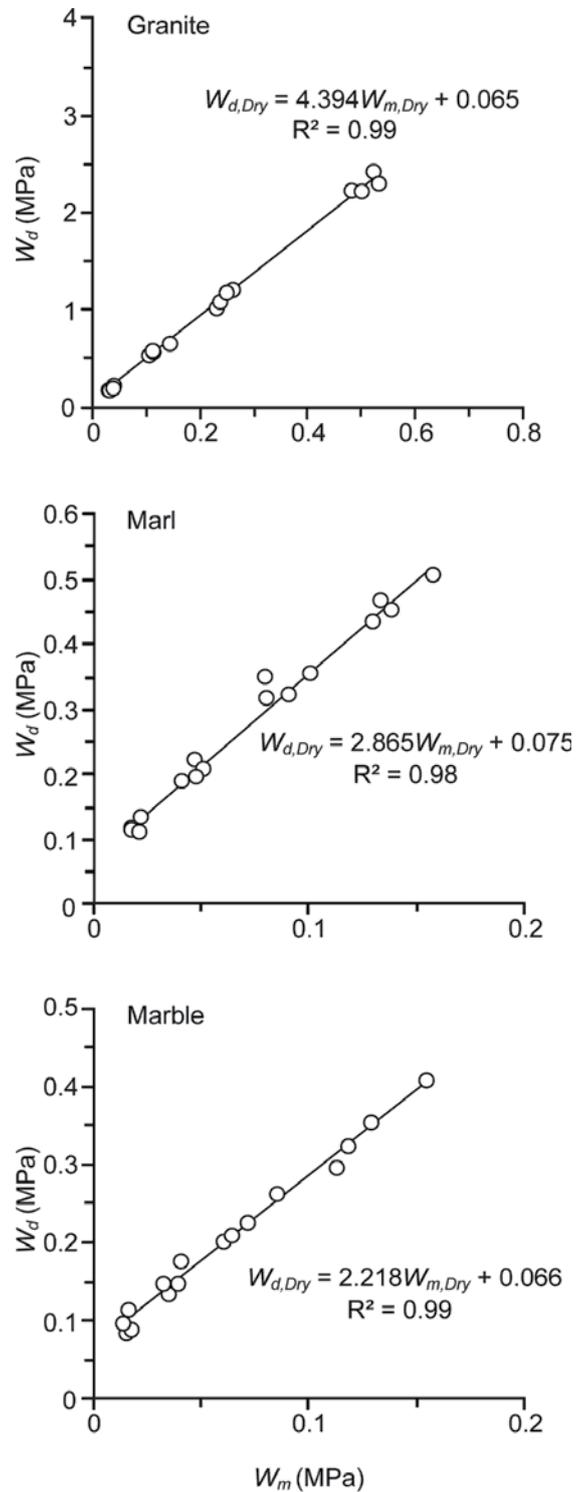
Figure 10 Distortional strain energy density $\left(W_d\right)$ at failure as a function of mean strain energy $\left(W_m\right)$ for dry specimens.

The cohesions of the dry and saturated specimens are comparable. The dry specimens yield slightly higher friction
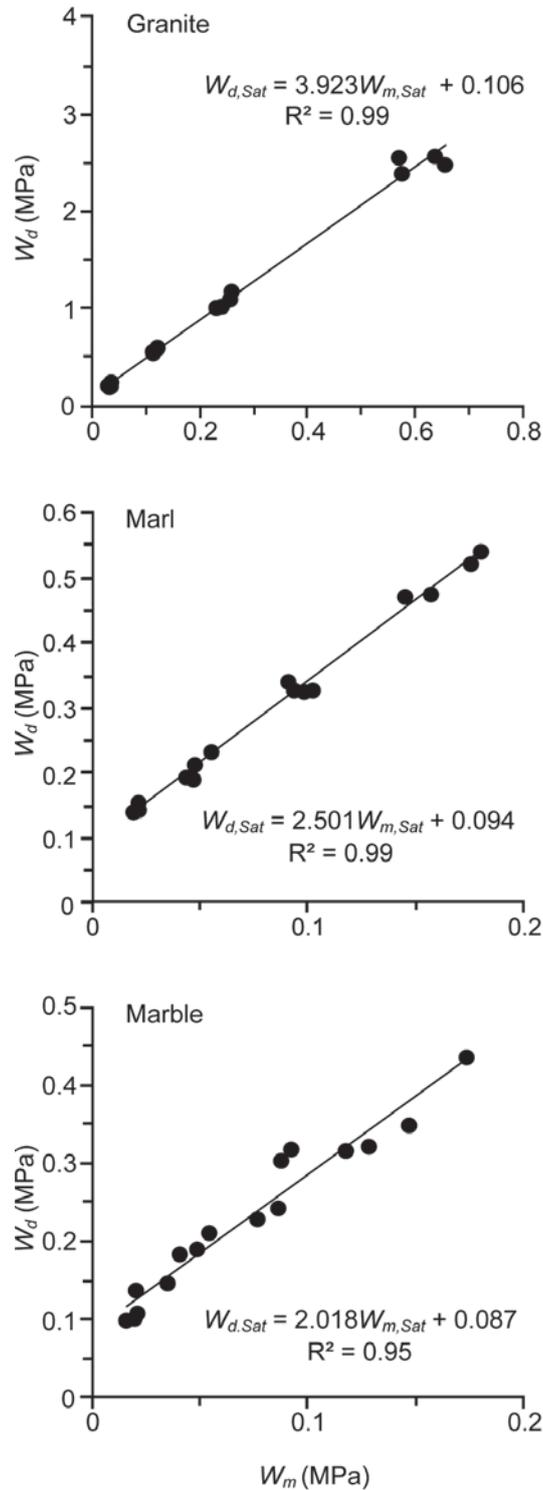
Figure 11 Distortional strain energy density (W_d) at failure as a function of mean strain energy (W_m) for saturated specimens.

angles than the saturated specimens. A multi–axial strength criterion is developed to describe the distortional strain energy density of rock at failure as a function of the mean strain energy. The energy required to fail the low porosity rocks under

dry condition is slightly higher than that under saturated condition. The distortional and mean strain energy is calculated from the principal stresses at failure and the rate-dependent elastic modulus. This means that if the total stresses and the loading rate are known, the proposed strength criterion can be used to predict the strength and deformation of in-situ rocks under dry and saturated conditions.

6. Acknowledgements

References

[1] A.Kumar, "The effect of stress rate and temperature on the strength of basalt and granite", Geophysic, 1968. Vol. 33, No. 3, pp. 501-510.

[2] I.W.Farmer, Engineering Behavior of Rock, 2nd Edn., Chapman and Hall, London.

[3] J.C.Jaeger, and N.G.W.Cook, Fundamentals of Rock Mechanics, 3rd Edn., Chapman and Hall, London.

[4] N.D.Cristescu, and U.Hunsche, Time Effects in Rock mechanics, John Wiley and Sons, New York.

[5] K.Masuda, "Effects of water on rock strength in a brittle regime", Journal of Structural Geology., 2001, Vol. 23, No. 11, pp. 1653-1657.

[6] B.Vasarhelyi, "Some observations regarding the strength and deformability of sandstones in case of dry and saturated conditions", Bulletin of Engineering Geology and theEnvironment, 2003, Vol. 62, pp. 245-249.

[7] A.Torok, and B.Vasarhelyi, "The influence of fabric and water content on selected rock mechanical parameters of travertine, examples from Hungary",
Engineering Geology, Vol. 115, pp. 237-245.

[8] J.Sun and Y.Y.Hu, "Time-dependent effects on the tensile strength of saturated granite at three gorges project in China", International Journal of Rock Mechanics and Mining Sciences., 1997, Vol. 34, No. 3-4, pp. 306.e1-306.e13.

[9] I.Yilmaz, "Influence of water content on the strength and deformability of gypsum", International Journal of Rock Mechanics and Mining Sciences., 2010, Vol. 42, No. 2, pp. 342-347.

[10] R.Yoshinaka, T.V.Tran and M.Osada, "Pore pressure changes and strength mobilization of soft rocks in consolidated-undrained cyclic loading triaxial tests", International Journal of Rock Mechanics and Mining Sciences., 1997, Vol. 34, No. 5, pp. 715-726.

[11] M.S.A.Perera, P.G.Ranjith and M.Peter, "Effect of saturation medium and pressure on strength parameters of Latrobe Valley brown coal: Carbon dioxide, water and nitrogen saturations", Energy, 2011, Vol. 36, No. 12, pp. 6941-6947.

[12] ASTM D4543-85. Standard practice for preparing rock core specimens and determining dimensional and shape tolerances, In Annual Book of ASTM Standards, 04.08, American Society for Testing and Materials, Philadelphia.

[13] K.Fuenkajorn, and N.Kenkhunthod, "Influence of loading rate on deformability and strength of three Thai sandstones", Geotechnical and Geological Engineering., 2010, Vol. 28, pp. 707-715.

[14] J.C.Jaeger, N.G.W.Cook and R.W.Zimmerman, Fundamentals of Rock Mechanics, 4th Edn., Chapman and Hall, London.